Conf-9108118--39

BNL-46794
CAP 77-91C

Analysis of a High Brightness Photo Electron Beam with Self Field and Wake Field Effects

Zohreh Parsa
Physics Department
Brookhaven National Laboratory
Upton, Long Island, New York 11973

CENTER FOR ACCELERATOR PHYSICS

BROOKHAVEN NATIONAL LABORATORY
ASSOCIATED UNIVERSITIES, INC.
Under Contract No. DE-AC02-76CH00016 with the
UNITED STATES DEPARTMENT OF ENERGY

DISTRIBUTION OF THIS DOCUMENT IS UNLIMITED

Presented at the Thirteenth International Free Electron Laser Conference
Santa Fe, NM, Aug. 25-30, 1991

DISCLAIMER

This report was prepared as an account of work sponsored by an agency of the United States Government. Neither the United States Government nor any agency thereof, nor any of their employees, nor any of their contractors, subcontractors, or their employees, makes any warranty, express or implied, or assumes any legal liability or responsibility for the accuracy, completeness, or usefulness of any information, apparatus, product, or process disclosed, or represents that its use would not infringe privately owned rights. Reference herein to any specific commercial product, process, or service by trade name, trademark, manufacturer, or otherwise, does not necessarily constitute or imply its endorsement, recommendation, or favoring by the United States Government or any agency, contractor or subcontractor thereof. The views and opinions of authors expressed herein do not necessarily state or reflect those of the United States Government or any agency, contractor or subcontractor thereof.

ANALYSIS OF A HIGH BRIGHTNESS PHOTO ELECTRON BEAM WITH SELF FIELD AND WAKE FIELD EFFECTS*

BNL--46794

DE92 004983

Zohreh Parsa

Brookhaven National Laboratory

Upton, New York 11973, U.S.A.

Abstract. High brightness sources are the basic ingredients in the new accelerator developments such as Free-Electron Laser experiments. The effects of the interactions between the highly charged particles and the fields in the accelerating structure, e.g. R.F., Space charge and Wake fields can be detrimental to the beam and the experiments. We present and discuss the formulation used, some simulation and results for the Brookhaven National Laboratory high brightness beam that illustrates effects of the accelerating field, space charge forces (e.g. due to self field of the bunch), and the wake field (e.g. arising from the interaction of the cavity surface and the self field of the bunch).

I. Introduction

The high brightness laser driven radio frequency (RF) cavities (Guns), are potential sources of high current, low emittance and short bunch beams of electrons, required for new methods of acceleration, such as (FEL) free electron Lasers. To achieve high brightness and rapid acceleration, a radio frequency gun operating at 2.856 GH, with 1 1/2 cell, π mode resonant, disc loaded structure (with cathode placed at the start of the first 1/2 cell), is designed and operating as the injector for the two S-bend LINAC sections at the BNL Accelerator Test Facility (ATF). This presentation includes, (in Section II), beam dynamics analysis of a high brightness beam of photoelectrons, with the RF, self-field and wake field effects on the particles in the cavity (e.g. BNL photo cathode gun). Formulation is discussed in Section III.

*Work performed under the auspices of the U.S. Department of Energy contract No. DE-AC02-76CH00016.

MASTER

DISTRIBUTION OF THIS DOCUMENT IS UNLIMITED

II. Beam Analysis

The BNL gun consists of a 1 1/2 cell π-mode cavity with a metal photocathode at the midplane of its first cell. With inner diameter of 83.08 mm, and total length of 78.75 mm (where the Ist cell length = 2.625 cm, and the 2nd cell length = 5.250 cm, with radius of aperture of 1 cm.

The gun is powered by a (conventional type), SLAC klystron, and is designed to produce a low emittance beam of 4.65 MeV at the exit of the gun, with the 100 MV/m field on cathode (i.e., an average axial gradient of 66.6 MV/m).

With laser spot size σ_r = 1.25 mm, laser pulse width σ_τ = 2Ps (.6 mm), charge of 0.9 nC, E_0 = 100 MV/m, when (initial phase) $\varphi_0 = 50°$ we obtain the max energy (4.21 MeV) and minimum transverse emittance (ϵ_T^N = 9.8 π-mm-mrad) at the gun exit ($Z \simeq 98$ mm). The bunch RMS length is 1.077 mm, RMS radius is 3.17 mm, longitudinal emittance (ϵ_L^N) is 4.55 mm-mrad and peak current is 188A. After magnetic compression, the bunch RMS length reduces to .967 mm and peak current increases to 212A. Variation in the exit parameters for the gun with respect to changes in the initial phase ϕ_0 is given in Figures 1–3. Figure 4 shows a schematic of the BNL photocathode gun, and Figures 5–12, the behavior of the beam (including RF, the space charge and wake-field effects) are shown at various points along the cavity.

Figures 1 show a)variations in the bunch RMS length; b) RMS radius; c) normalized transverse ; and d) normalized longitudinal emittance respectively, with respect to variation in the initial phase angle.

Figures 2 (a–d), show a) variation in peak current, b) bunch RMS length after magnetic compression, d) bunch average kinetic energy with variations in initial phase angle.

Figures 3 (a–b), show a) % RMS $\delta\gamma/\gamma$, and b) shows the RMS Divergence with variation in phase angle.

Figure 4 shows a sketch of the BNL photocathode gun. Since lowest emittance and highest momentum occurs when the initial phase angel is 50°, in Figures 5–12, we illustrate effects of wake and self field on the beam.

Figure 5 shows the effect of the wake and bunch self field.

Figure 6 shows the propagation of self-field.

Figure 7 shows H_ϕ field with respect to R.

Figure 8 is plot of J_r and J_z distributions as functions of z.

Figure 9 shows constant field lines around the bunch.

Figure 10 shows the transverse phase space plot of $x - x'$ (at $z = 98$ mm).

Figure 11 shows the phase space plot of P_z vs z at $z = 98$ mm.

Figure 12 shows variations of the charge density-divE with respect to Z and R.

III. Formalism

In this section we present a brief overview of the formalism used to study the interaction of highly charged particle bunches with the fields inside the accelerating structures, e.g., the BNL photocathode gun (illustrated in Section II).

An initial driving current $\vec{J} = (J_r(r,z,t), J_z(r,z,t))$ in presence of a TM-Field, ($H\phi$, Er, Ez), form a "self-consistent" set of equations:

$$\nabla^2 \vec{H} - \frac{1}{c^2}\frac{\partial^2 \vec{H}}{\partial t^2} = -\nabla \times \vec{J} \tag{1}$$

and

$$\frac{d\vec{p}}{dt} = q\left(\vec{E} + \vec{v} \times \vec{B}\right) \tag{2}$$

$\vec{v} = (v_r, v_z)$, the fields $\vec{E} = E(r,z,t)$ $\vec{H} = H(r,z,t)$; and the source $J = J(r,z,t)$ and $\vec{\rho} = \vec{\rho}(r,z,t)$ are axisymmetrical. Where the scalar equation $L\phi = \frac{1}{c^2}\frac{\partial^2\phi}{\partial t^2} - r\frac{\partial J_z}{\partial r} - r\frac{\partial J_r}{\partial z}$ gives the time evolution of the fields, $L \equiv \frac{\partial^2}{\partial z^2} + \frac{\partial^2}{\partial r^2} - \frac{1}{r}\frac{\partial}{\partial r}$, and the pseudo scalar potential $\phi = rH_\phi$; $H_\phi = H_\phi(r,z,t)$.

The driving current is due to the motion of the bunch of particles around the axis of cavity, and since the deriving current must be axisymmetrical the particles (of the bunch) can only move in the r - z plane; (so their charge density and current are the same as those produced by "rings of charge" centered on - axis); can move axially or expand radially.

There are various ways of solving these equations, one way is to use the standard Finite Difference Method (FDM) that allows the transform of the differential problems into the algebraic ones, via the discretization of the operators (L) and functions (ϕ, Jr, Jz), over a mesh. In that one solves simultaneously the equations for the field propagation and the equation of motion for the particles.

Thus the effects of the e.m. interactions on the beam dynamics properties, such as emittances, energy spreads, etc. can be obtained [4], knowing the field H_ϕ at each mesh point at present and at next integration time, the equation is integrated with respect to the standard R. K. method. with the charge distribution

$$\rho_i(r, r_i, z, z_i) = e^{-\frac{(z-z_i)^2}{2\sigma_z^2} - \frac{(r-r_i)^2}{2\sigma_r^2}} e^{-\left(\frac{r\, r_i}{\sigma_r^2}\right)}$$
$$\alpha_{0i} = \frac{q_i}{(2\pi)^{3/2}\,\sigma_r^2\sigma_z} \bullet I_0\left(\frac{r\, r_i}{\sigma_r^2}\right) \tag{3}$$

the corresponding current densities are:

$$J_z = \beta_{\|}^i \alpha_{0i} e^{-(z-z_i)^2/2\sigma_z^2} e^{(-r^2-r_i^2)/2\sigma_r^2} \tag{4}$$

$$J_r = \beta_{\perp}^i \alpha_{1i} e^{-(z-z_i)^2/2\sigma_z^2} e^{(-r^2-r_i^2)/2\sigma_r^2} \tag{5}$$

which satisfy the continuity equation, guarantees gauge invariance ($\nabla \bullet \vec{E} - \rho/\varepsilon = 0$) and minimizes the unphysical fluctuation in the driving current.

In equations (3–5), σ_r, σ_z are the charge and coordinates of the i-th particle; $\beta_{\perp i}$ and $\beta_{\|i}$ are the radial and axial components of the i-th particle beta respectively; I_0 and I_1 are the 0-th and 1st-order modified Bessel function of the first kind; and $\alpha_{1i} = \frac{q_i c}{(2\pi)^{3/2}\sigma_r^2\sigma_z^2} I_1(\frac{r\, r_i}{\sigma^2})$. (For detailed formulation see references.)

<u>On Emittance:</u> For clarity, we note the following emittance definitions are used in this analysis; Normalized Transverse Emittance $= \sqrt{x^2 p_x^2 - (x\ p_x)^2}$, ($\epsilon_T^N$) and RMS Transverse Emittance $= \sqrt{x^2 x'^2 - (x\ x'^2)}$, (for discussion of emittance including higher order moments see [5]).

IV. Summary

We illustrated the interaction between the self-field and wake field induced in the cavity for the BNL RF gun photoelectron beam. We used $\sigma_R = 1.25$ mm, (a smaller radius than the designed value of 3.00 mm) to reduce the beam loss at the gun exit. This smaller σ_R value was also indicated by the preliminary measured data at ATF. Our studies show, the initial phase $\varphi_0 = 50°$ results in the optimum values for the beam exit parameters. Additional information is given in References [1–7], e.g. the effects of variation in laser pulse length is given in Ref. [6], our analysis with PARMELA in Ref. [3], some of the preliminary data from ATF is also given in this proceeding.

References

[1] Z. Parsa, *Preliminary emittance measurements and calculations of the laser excited beam from the BNL ATF RF electron gun*, Proc., BNL CAP Meetings, Vol. II, BNL-52292 (1991).

[2] K. Batchelor, K. McDonald *et al.*, Proc., EPAC88, June 1988.

[3] Z. Parsa and L. Young, this conference.

[ ] Z. Parsa, L. Serafini, (in press) 1991. L. Serafini, C. Pagani, Proc. EPAC, Nile Ed., Frontieres, (1990); Private Communication, Code ITACA, L. Serafini, A. Pretti.

[5] Z. Parsa, Proc. EPAC, Nile Ed., Frontieres, (1990) and Ref. therein.

[6] Z. Parsa, this conference.

[7] Z. Parsa, Proc. of PF91 Conf., Vancouver, Canada, (Aug. 1991).

Figure Captions

Figures 1 a) Variations in the bunch RMS length; b) RMS radius; c) normalized transverse; and d) normalized longitudinal emittance respectively, with respect to variation in the initial phase angle.

Figures 2 a) Variation in peak current; b) bunch RMS length after magnetic compression; d) bunch average kinetic energy with variations in initial phase angle.

Figures 3 a) % RMS $\delta\gamma/\gamma$; and b) shows the RMS Divergence with variation in phase angle.

Figure 4 Sketch of the BNL photocathode gun. Since lowest emittance and highest momentum occurs when the initial phase angel is 50°, in Figures 5–12, we illustrate effects of wake and self field on the beam.

Figure 5 Effect of the wake and bunch self field.

Figure 6 Propagation of self-field.

Figure 7 H_ϕ field with respect to R.

Figure 8 Plot of J_r and J_z distributions as functions of z.

Figure 9 Constant field lines around the bunch.

Figure 10 Transverse phase space plot of $x - x'$ (at $z = 98$ mm).

Figure 11 Phase space plot of P_z vs z at $z = 98$ mm.

Figure 12 Variations of the charge density-divE with respect to Z and R.

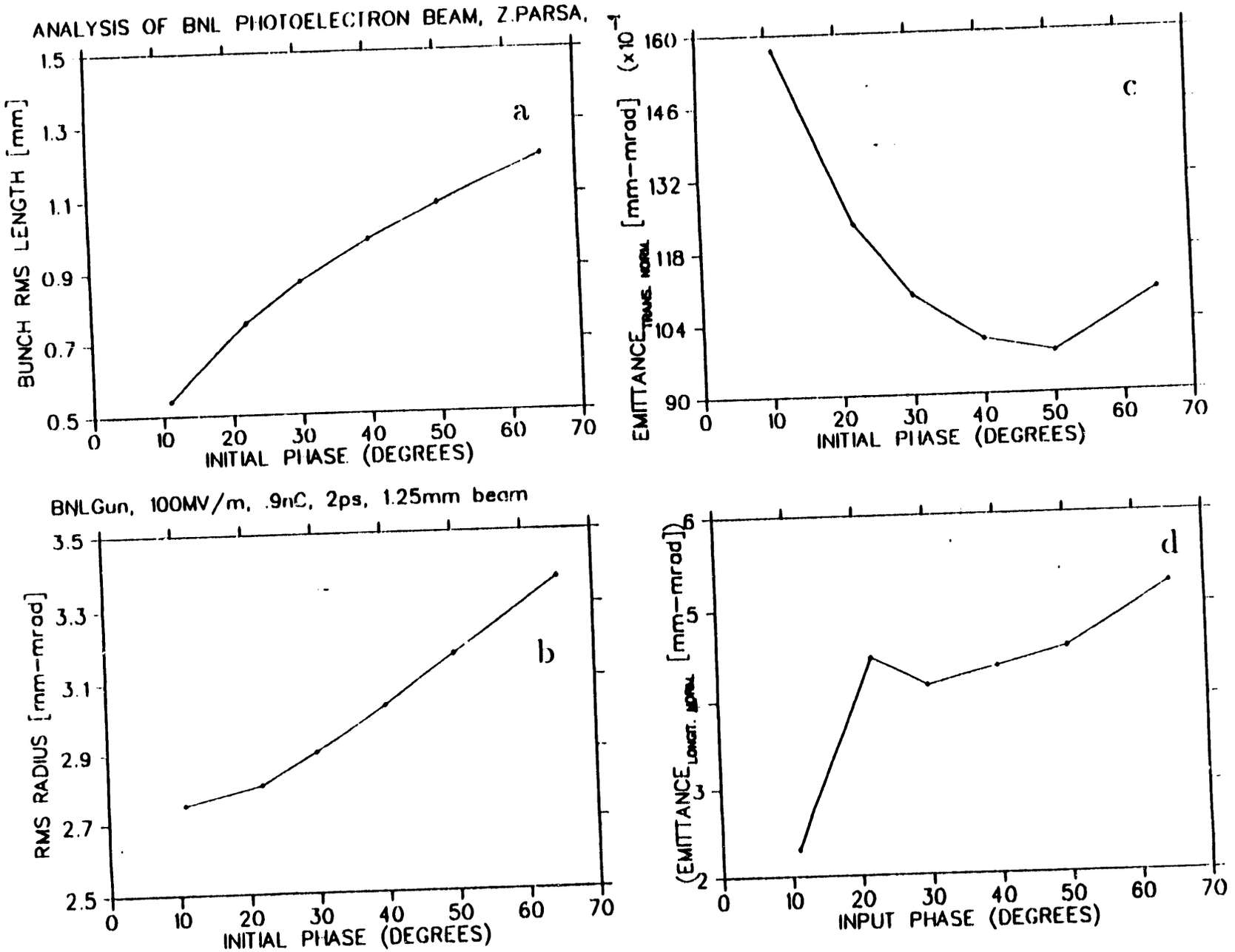
ANALYSIS OF BNL PHOTOELECTRON BEAM, Z.PARSA,
BNLGun, 100MV/m, .9nC, 2ps, 1.25mm beam
a
b
c
d
BUNCH RMS LENGTH [mm]
RMS RADIUS [mm-mrad]
EMITTANCE TRANS. NORM. [mm-mrad] (x10^-1)
(EMITTANCE LONGT. NORM. [mm-mrad])
INITIAL PHASE (DEGREES)
INPUT PHASE (DEGREES)

Figs. 1

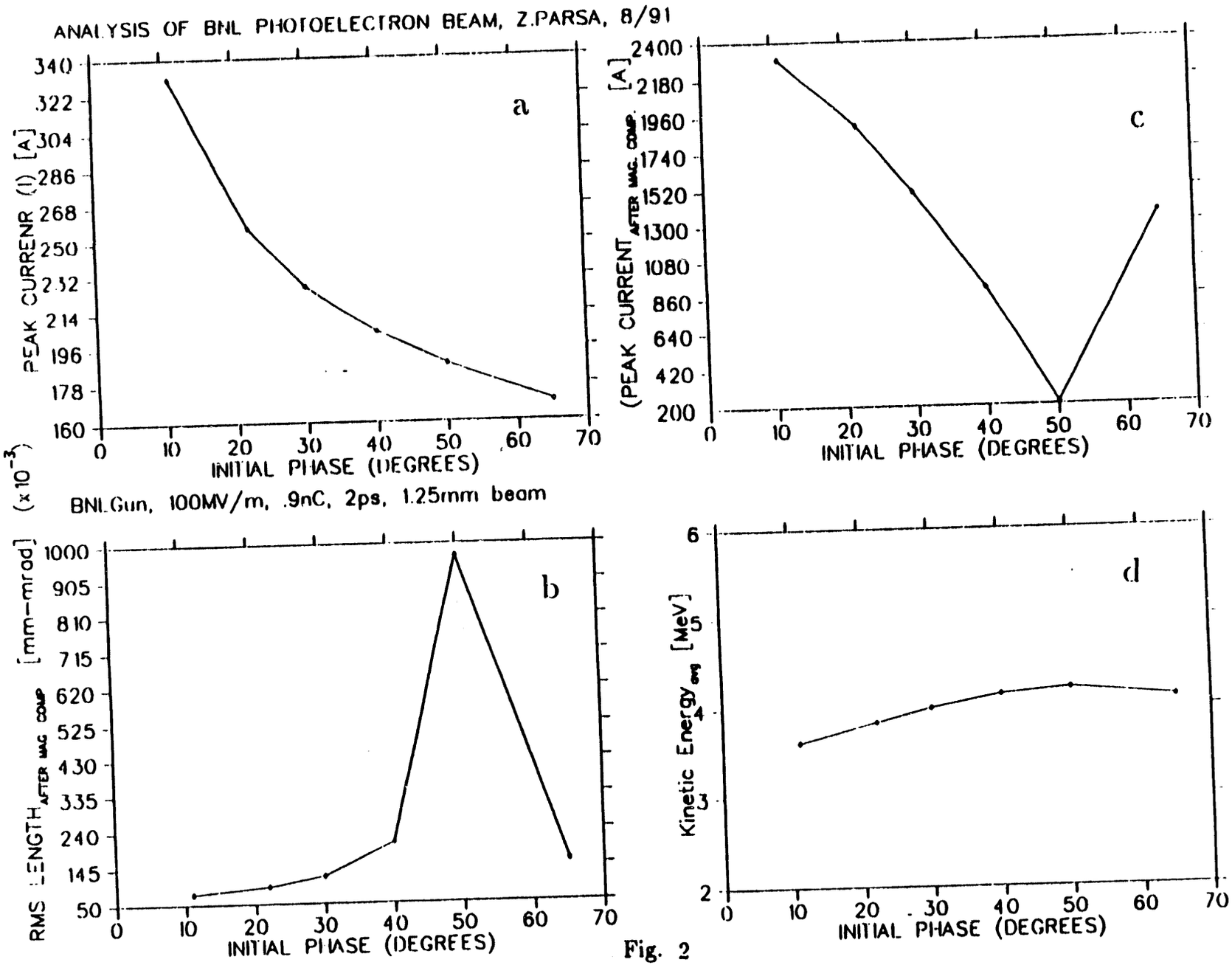
ANALYSIS OF BNL PHOTOELECTRON BEAM, Z.PARSA, 8/91
a
PEAK CURRENR (I) [A]
INITIAL PHASE (DEGREES)
c
(PEAK CURRENT AFTER MAG. COMP. [A]
INITIAL PHASE (DEGREES)
BNL Gun, 100MV/m, .9nC, 2ps, 1.25mm beam
b
RMS LENGTH AFTER MAG COMP [mm-mrad] (x10^-3)
INITIAL PHASE (DEGREES)
d
Kinetic Energy avg [MeV]
INITIAL PHASE (DEGREES)

Fig. 2

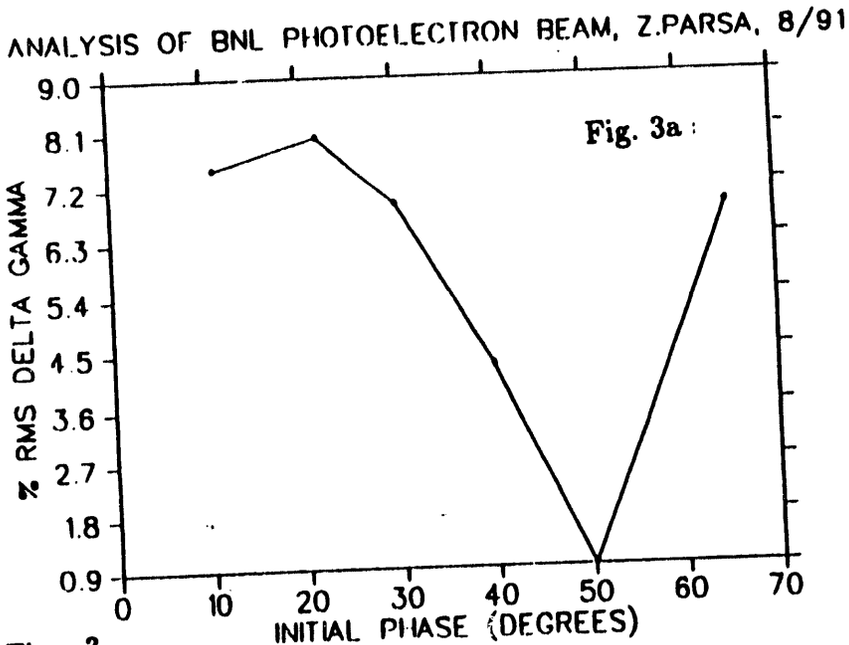

Fig. 3

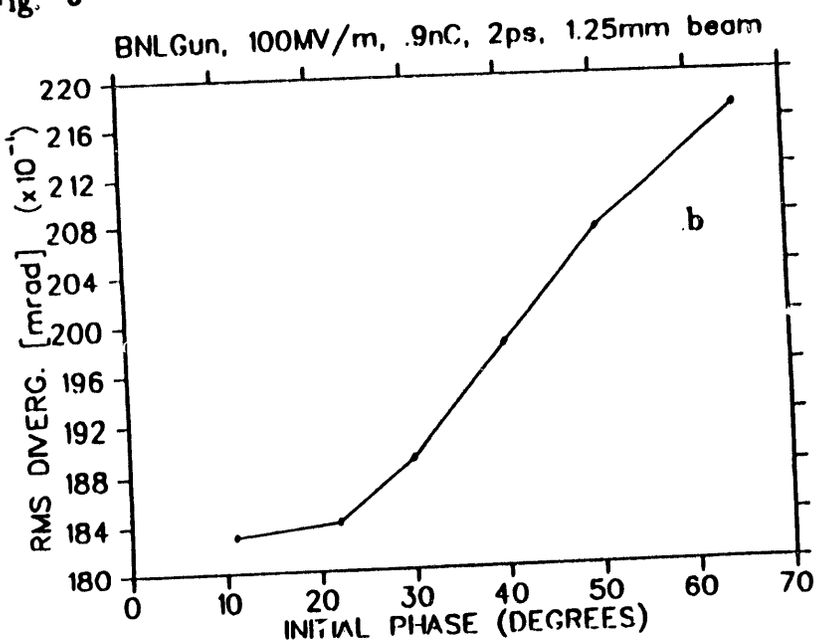

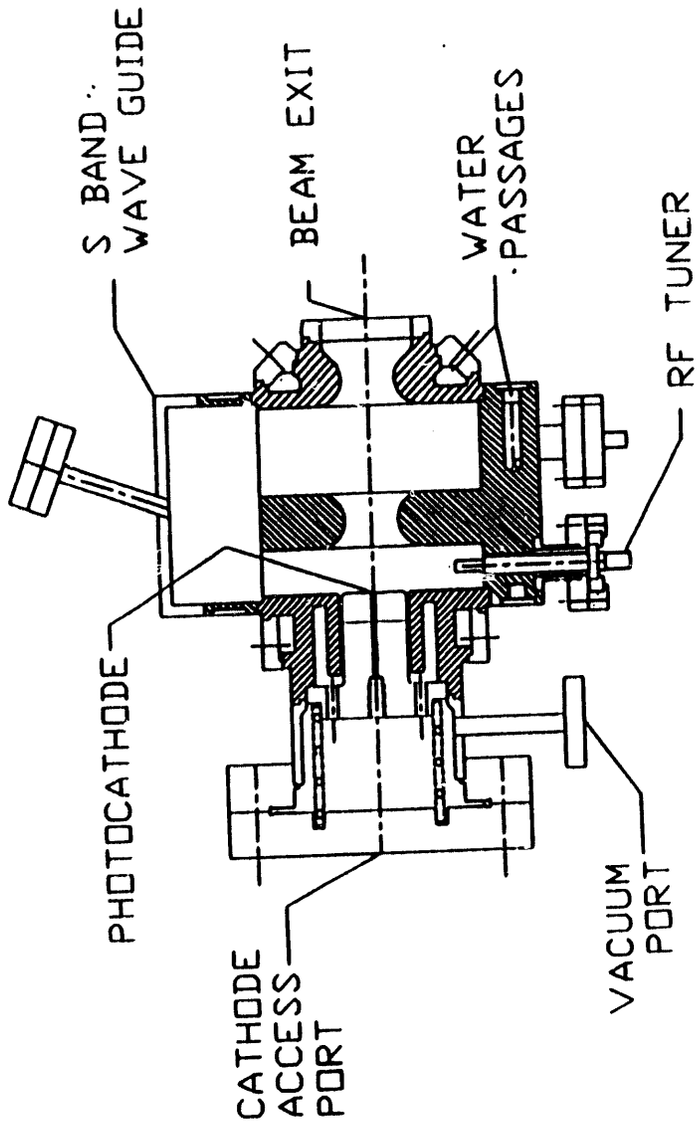

Fig. 4
BNL-RF gun

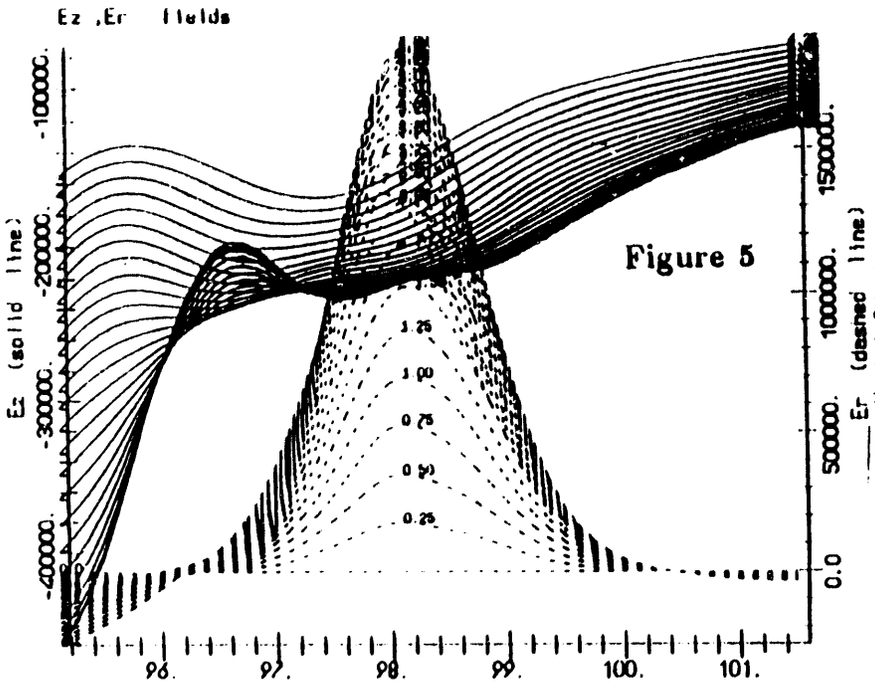

Figure 5

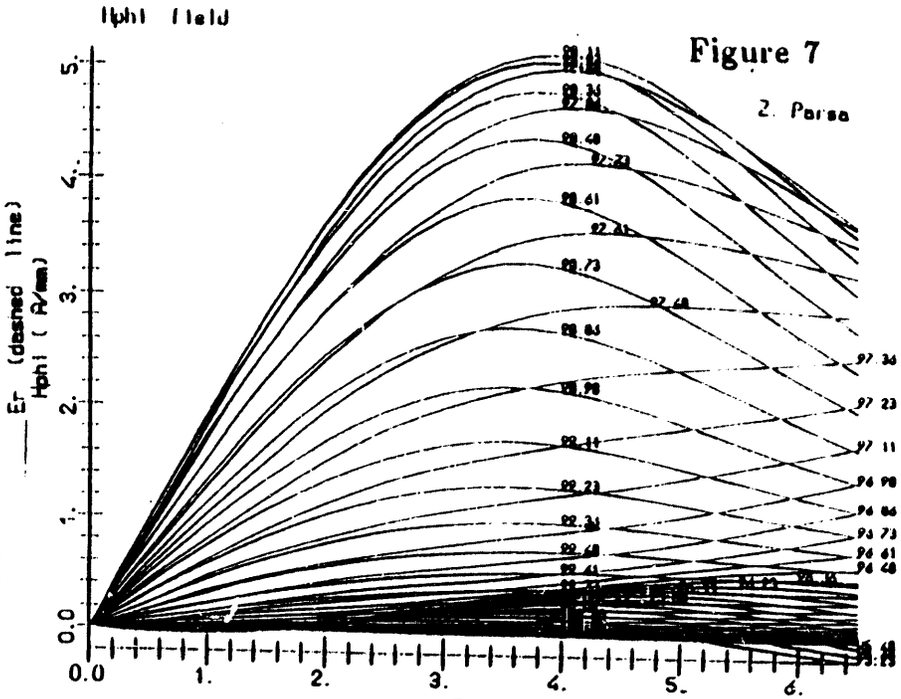

Figure 7

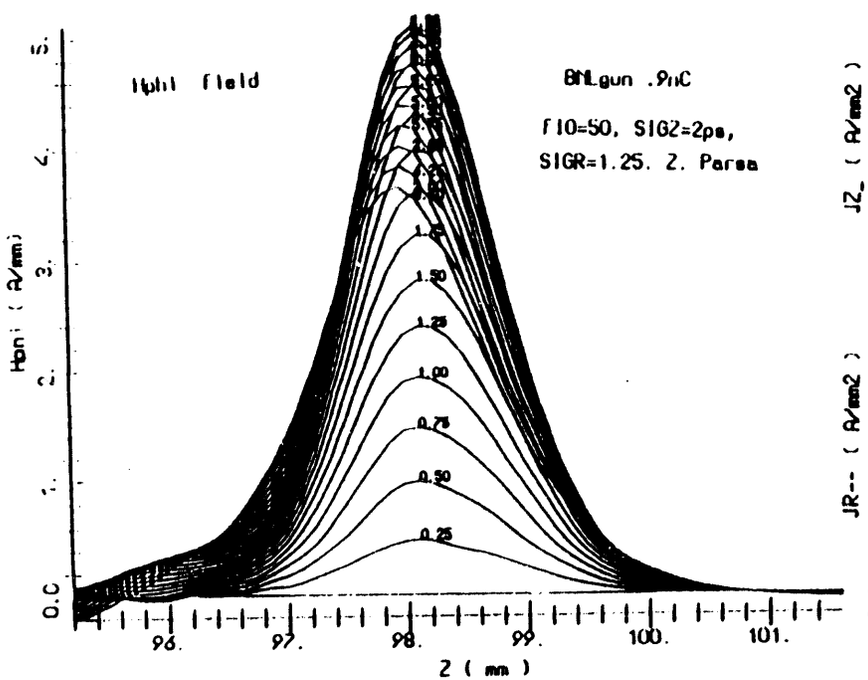

Figure 6

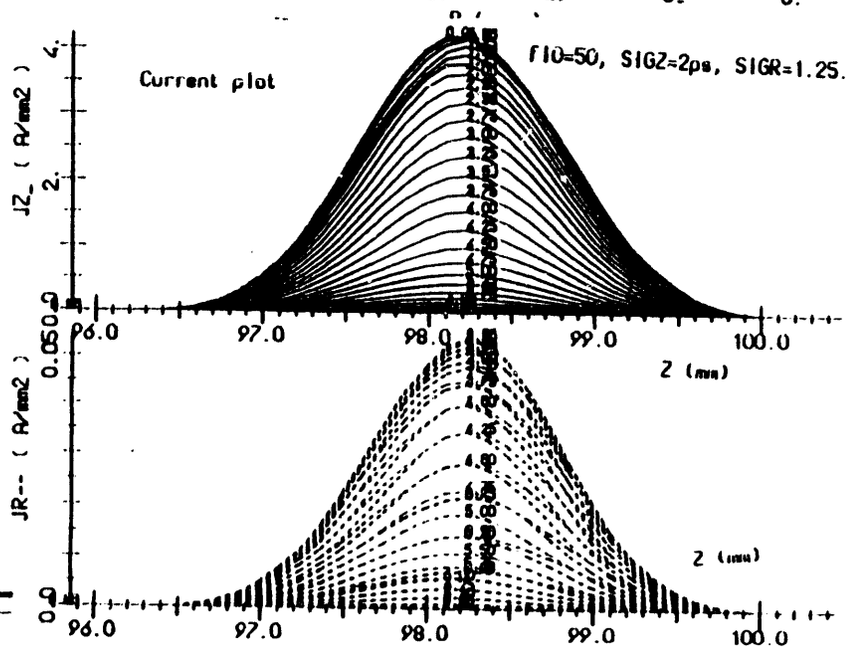

Figure 8

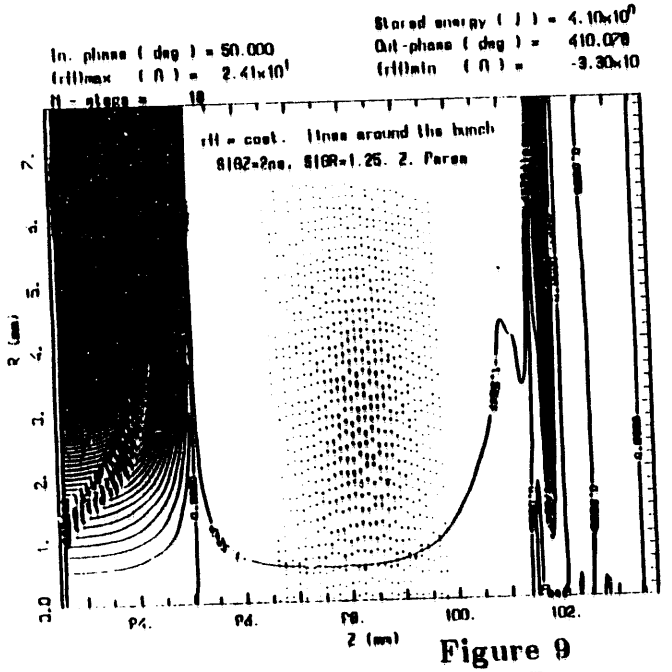

Figure 9

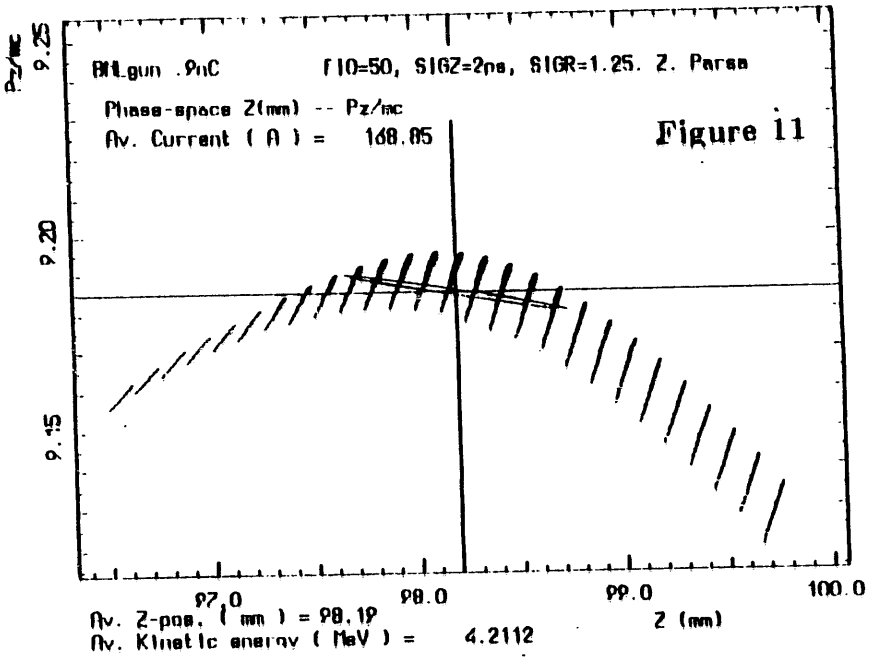

Figure 11

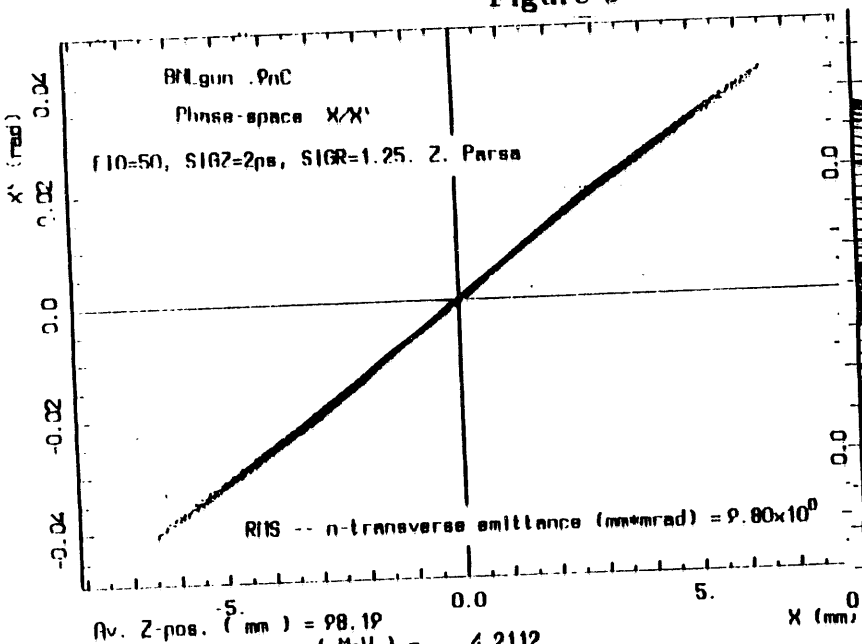

Figure 10

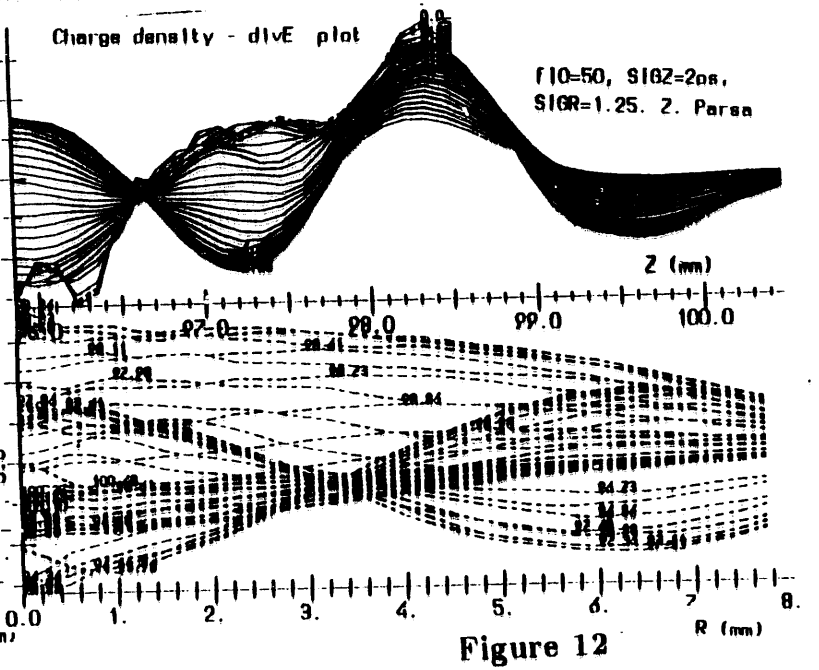

Figure 12

END

DATE FILMED

2 / 18 / 92